Short Term Mobility CNR **May 11 - June 18, 2014**

CNR IRPI Torino (Italy) - USGS Golden, CO (USA)

REPORT: a new debris-flow and rock-fall seismic monitoring station at Chalk Cliffs, CO

Velio COVIELLO - velio.coviello@irpi.cnr.it

May 22, 2014 - Installation

On May 22, 2014 two seismic sensors have been installed in the Chalk Cliffs basin, at the upper station of the already existing monitoring system designed by the USGS and composed by rain gauges, video cameras, stage sensors, force plates (Coe et al., 2008). The sensors are 4.5 Hz triaxial geophones made by Geospace and assembled by the Italian company Solgeo (Figure 1). The working frequency range of the sensors supposed to be flat is 8 ÷ 500 Hz, this latter maximum value has been derived through some tests performed in laboratory. The sensors transduction constant is equal to 32 V/m/s and the polarity is positive for movements in the axis directions for x- and y- axis, while is negative for z-axis. See Table 1 for the complete geophone's specifications.

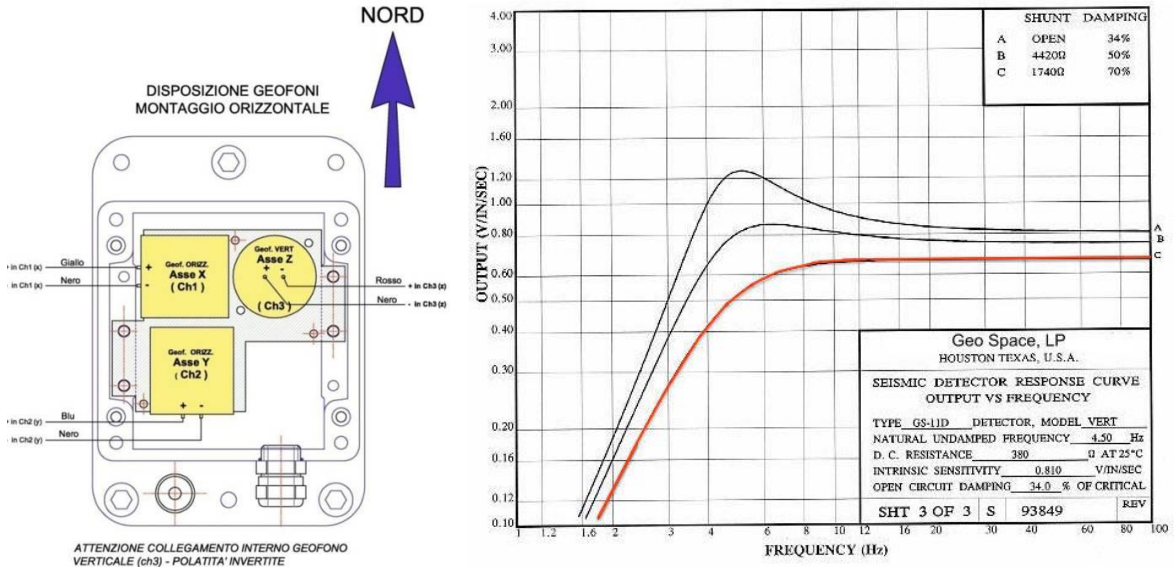

Figure 1 – The geophone scratch (left) and response curve (right, in red).

The downstream sensor (geophone A) has been screwed on the vertical face of a stable block located on the left bank of the channel, the other one (geophone B) is installed on the ground at the bridge section, on the right bank of the channel (Figure 2).

Table 1 – Specifications of the geophones.

Model	Solgeo VELOGET.3D
Number of axis	3, orthogonally oriented
Sensor	Geospace GS-11D 4.5 Hz
Case to coil motion	2,5 mm (p-p)
Damping	0.7
Voltage Sensitivity	32 V/m/sec
Housing	Aluminum
Protection	IP 65
Dimension	150 mm, 100 mm, 75 mm
Weight	1,6 Kg
Connection	Metallic connector o integrated cable
Accessories	Platform whit leveling screws, single bolt fixing

Figure 2 – The geophone A (left) at the downstream station and the geophone B (right) installed at the bridge section.

May 29, 2014 – First field test

On May 29, we collected one hour of recordings after the connections between the data logger (Campbell CR5000) and the geophones were set up. In particular, hereinafter are presented the signal (Figure 3) and the spectrogram (Figure 4) related to an induced rock fall of a block moved from the left bank and failed into the main channel rolling alongside the sensor.

In the time domain plot is possible to observe some first low intensity signal, due to the operator, which was moving on the ridge. These signals, mainly visible on the x- and z-axis, get maximum values of around 2 mV. After some seconds of silence the signal progressively starts rising.

The signal related to the block movements and impacts lasts around 3 minutes and the maximum amplitude level (around 90 mV) is reached on the vertical axis. On this latter channel the main signal frequency content is included in the range 50-150 Hz while on the x-axis seems to be a bit higher. In Figure 5 is presented the spectrogram derived from the signal likely related to the main impact.

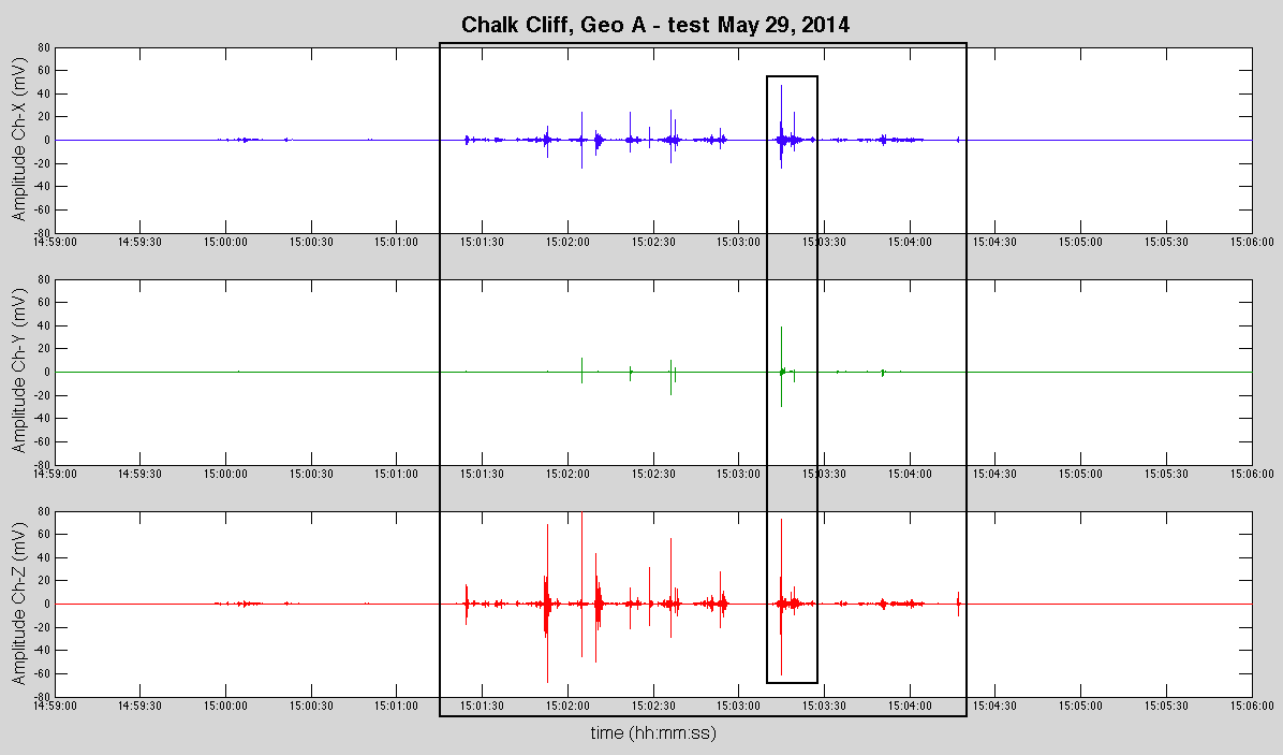

Figure 3 – The signal in time domain of the May 29 induced rock fall from the left bank (geophone A), the black frames contain the time intervals analyzed in frequency domain in Figure 4 and 5.

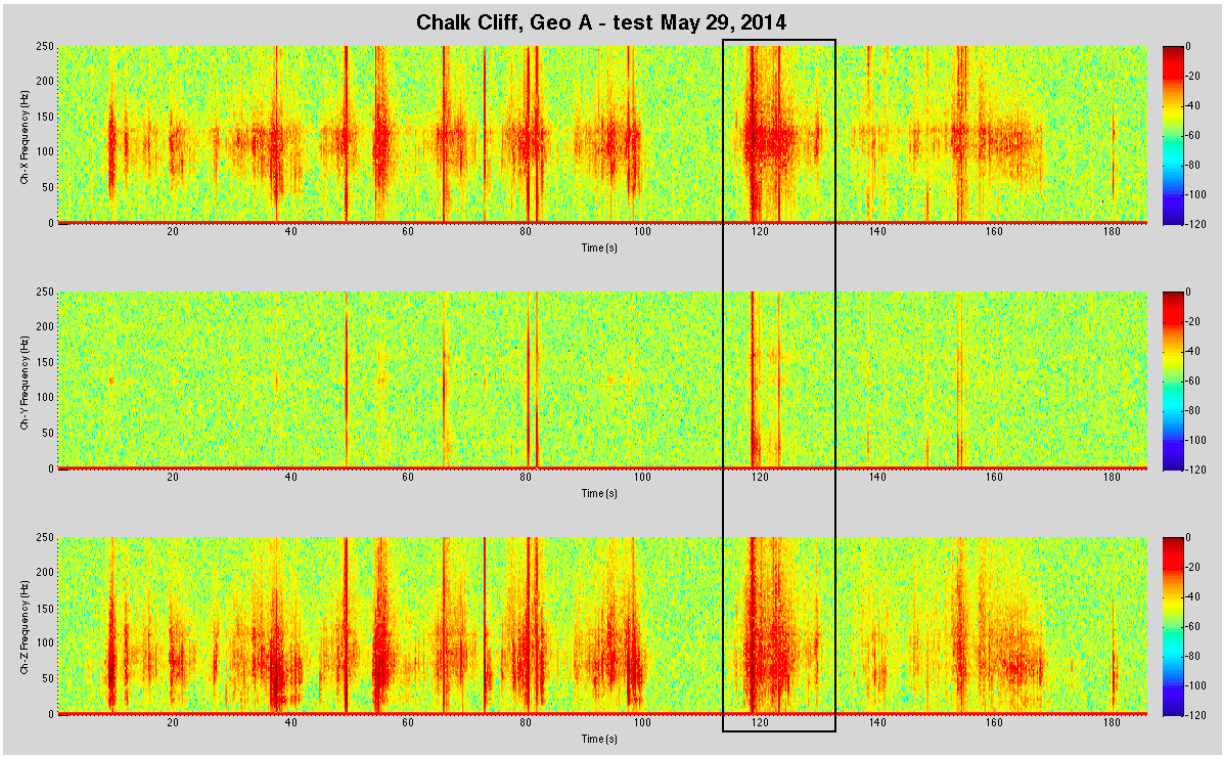

Figure 4 – The spectrogram of the May 29 induced rock fall from the left bank (geophone A), the black frame contains the portion of the spectrogram related to the main block impact enlarged in Figure 5.

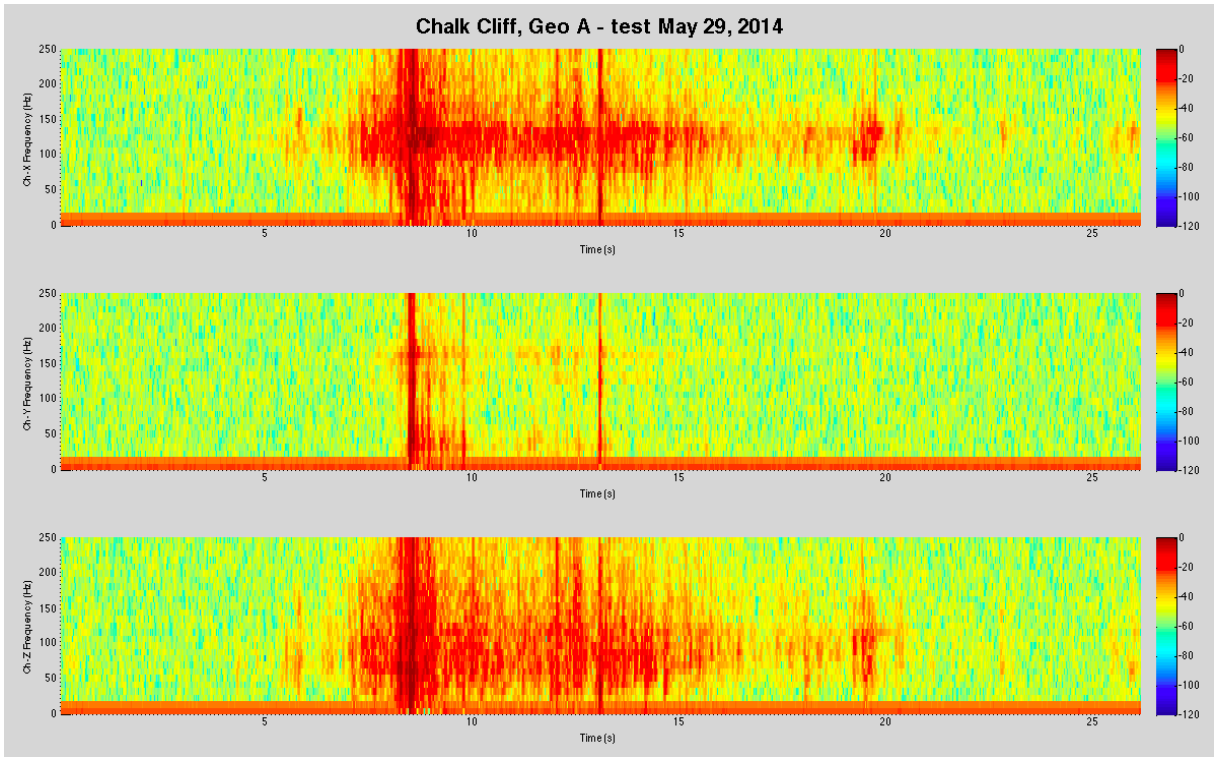

Figure 5 – The spectrogram of the May 29 induced rock fall from the left bank (geophone A.

June 6, 2014 – New field tests

We carried out a second series of tests on June 6, 2014 producing some controlled rock impacts and graveling along the channel banks. In Figure 5 and Table 2 a sketch and a summary of the tests location and characteristics are reported. Then, the seismograms recorded by the two sensors (Figure 6 and 7) are presented. Afterwards we focus on two specific events, a rock impact performed on the right bank (Figures 8 and 9), registered by the geophone B, and the raveling produced on the left bank (Figures 10 and 11), recorded by the geophone A. The signals related to these latter phenomena are presented, together with the spectrograms calculated on the investigated time intervals. The waveforms related to the two phenomena are rather different. In time domain, the rock impact produces short impulsive signals while the raveling determinates longer fluctuations. In frequency domain, the rock impact covers the whole frequency range, while the raveling is mainly recorded by the x- and the z- axis in a limited frequency band. Furthermore, in Figure 11 is possible to observe some vertical bands which are similar to the spectrogram presented in Figure 9; these signals are likely dues to the impact of the larger gravel.

Table 2 – Tests time and type, see Figure 5 for the sections location.

Time (hh:mm:ss)	Section		Type
12:27:56 12:28:26 12:29:05	1	Right Left Middle	~ 1 kg rock fall
12:29:42 12:30:00 12:30:15	2	Right Left Middle	~ 1 kg rock fall
12:31:25 12:32:06 12:32:21	3	Right Left Middle	~ 1 kg rock fall
12:32:53 12:34:02 12:34:21	4	Right Left Middle	~ 1 kg rock fall
12:35:45	4	Middle	~ 10 Kg rock fall downstream
12:36:55 - 12:38:10	4	Left	Raveling
12:40:00 - 12:42:00	3	Right	Raveling
12:43:00 - 12:44:30	3	Left	Raveling
12:45:17	3	Left	~ 10 kg rock fall downstream

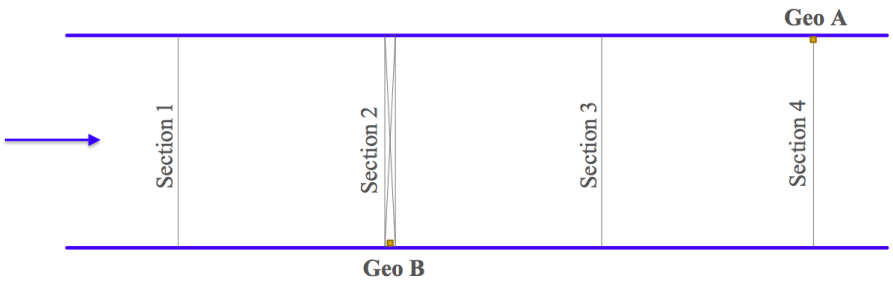

Figure 5 - Sketch of the geophones and the test sections location in the main channel.

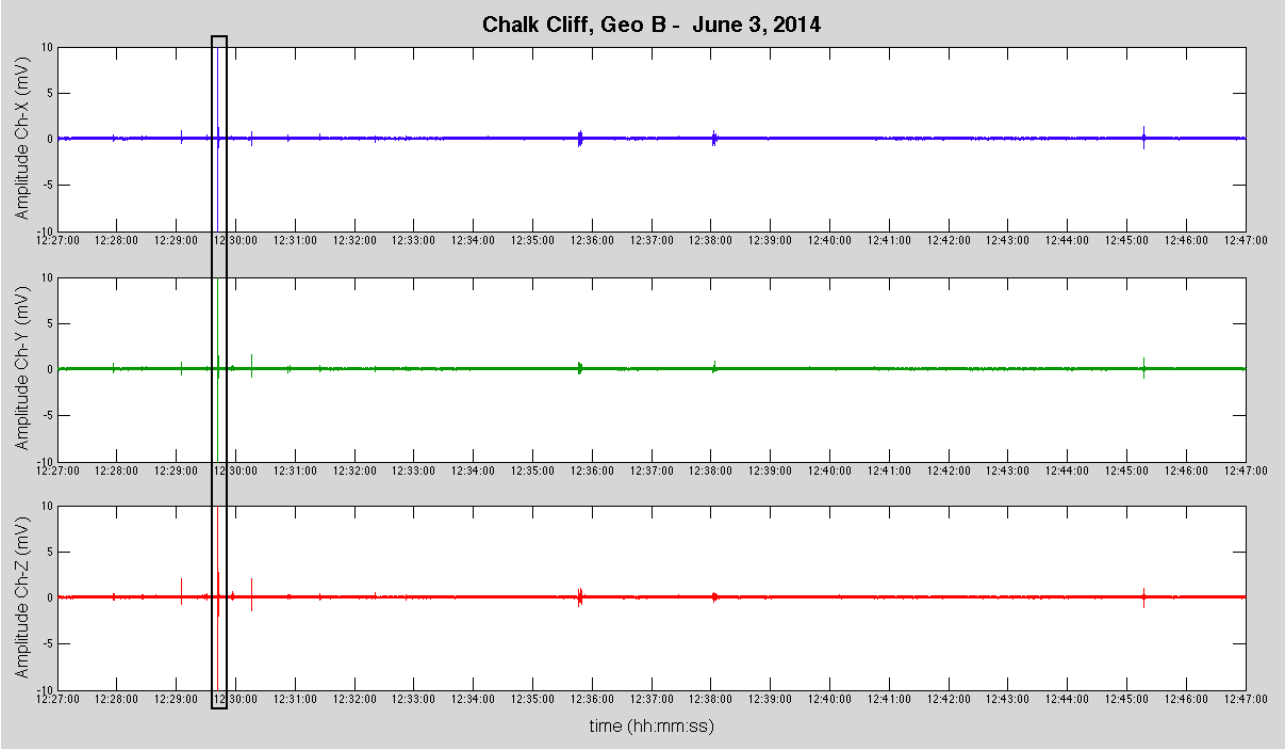

Figure 6 - The whole signal in time domain recorded by geophone B during the tests. The y-axis limits have been took in to emphasize the waveforms, the black frame contains the portion of the signal enlarged in Figure 7.

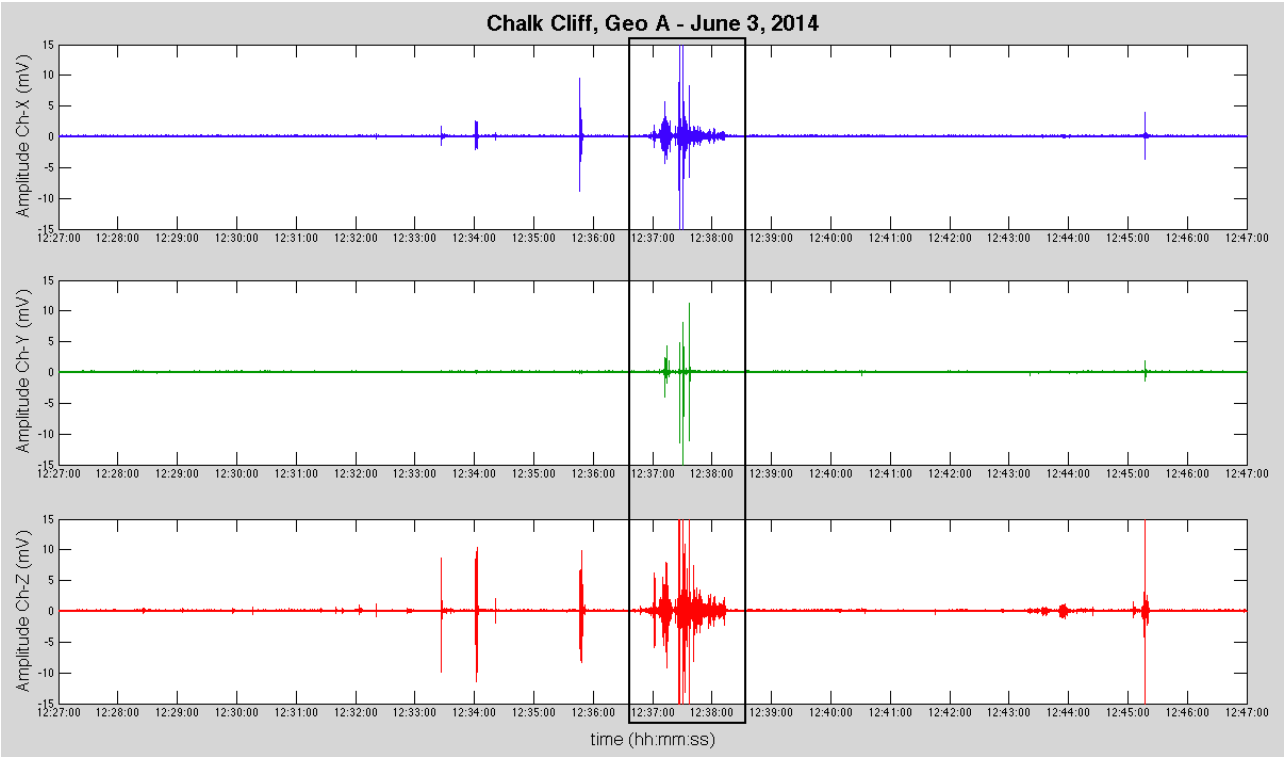

Figure 7 - The whole signal in time domain recorded by geophone A during the tests. The y-axis limits have been took in to emphasize the waveforms, the black frame contains the portion of the signal enlarged in Figure 10.

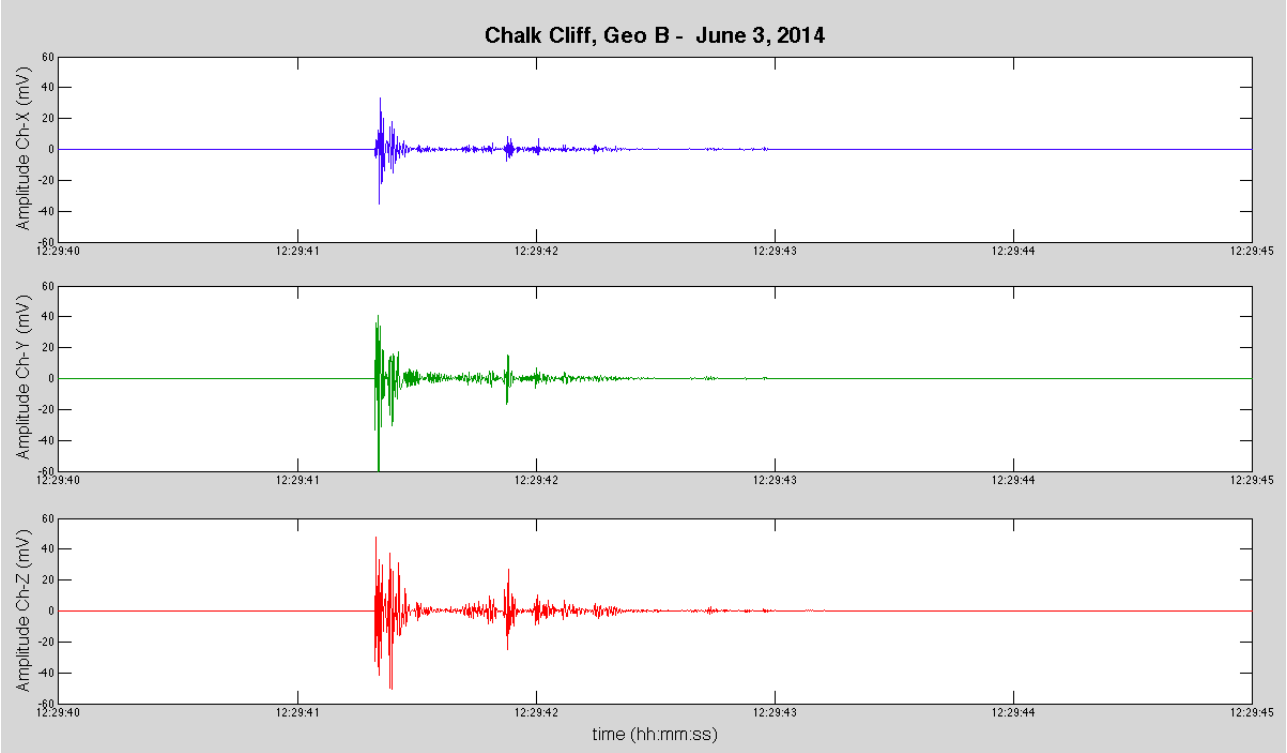

Figure 8 - The signal in time domain (zoom of Figure 6) of the rock fall test conducted on the right bank (section 2) and recorded by the geophone B.

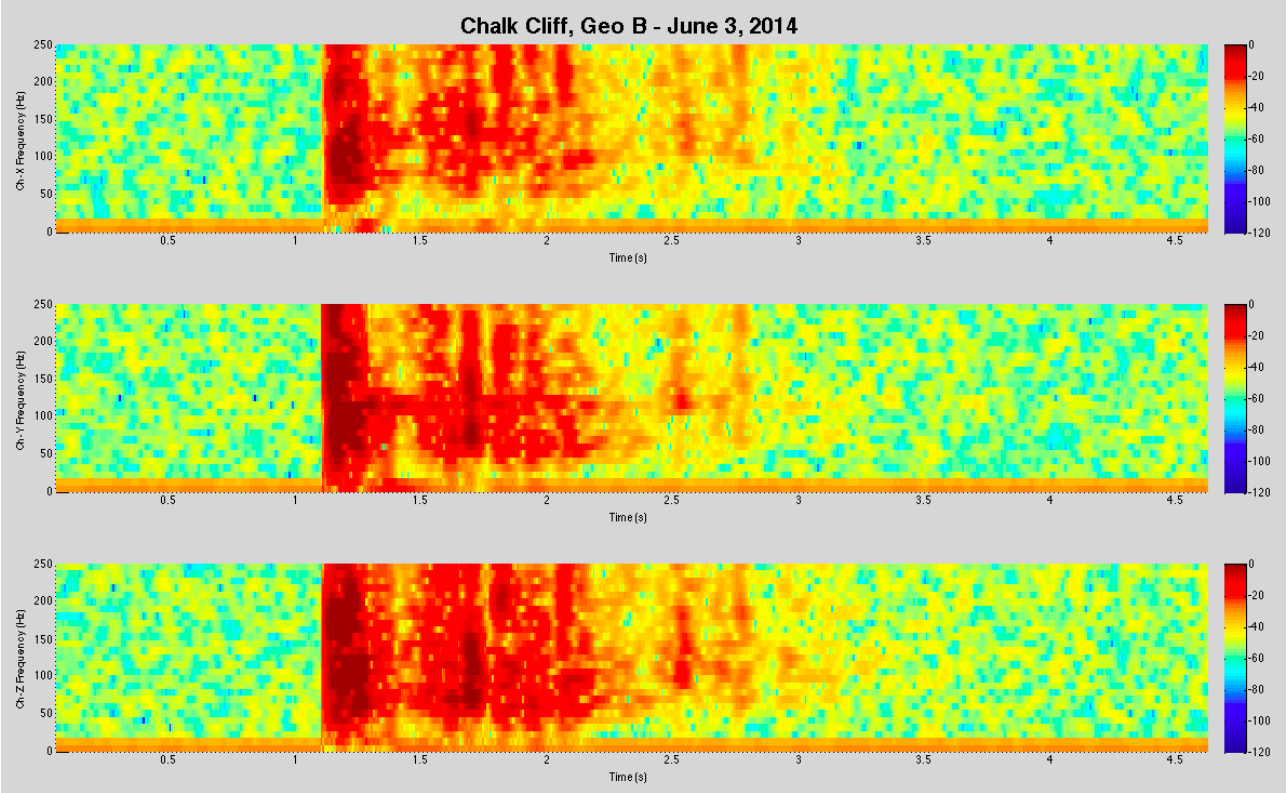

Figure 9 - The spectrogram of the rock fall test conducted at 12:29:43 (section 2) and recorded by the geophone B.

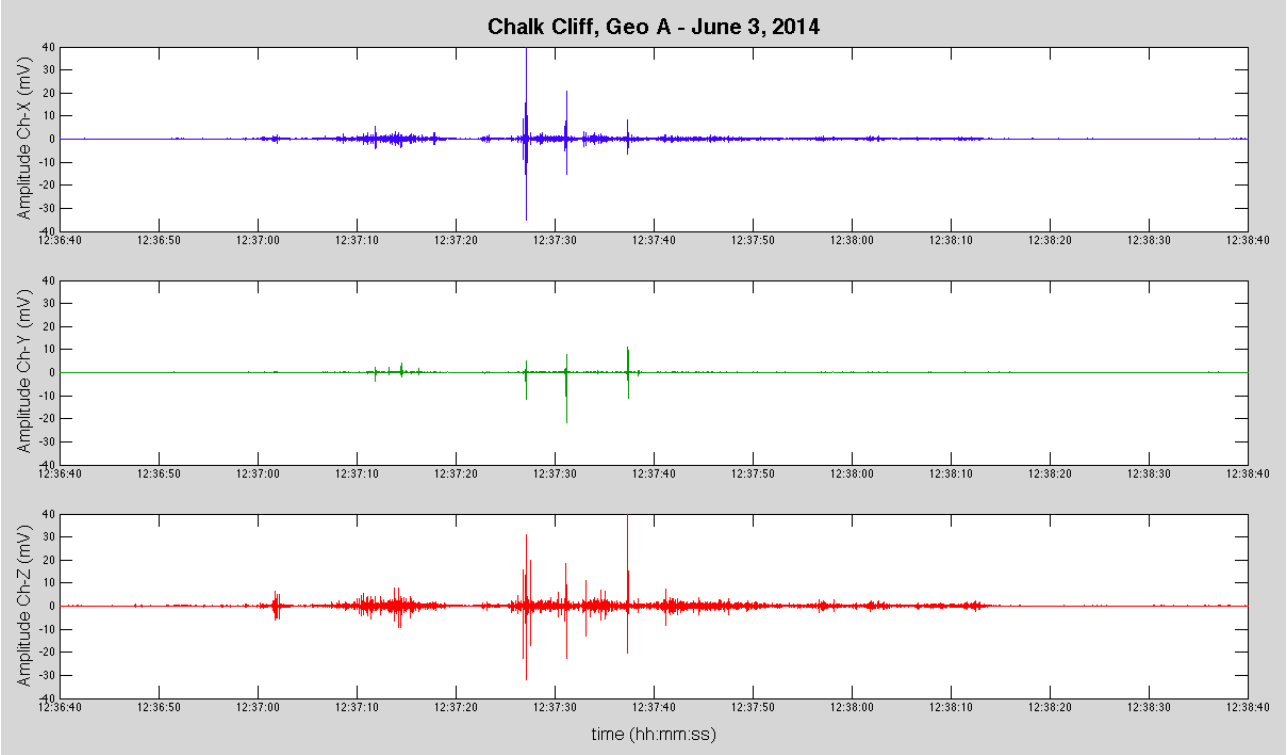

Figure 10 - The signal in time domain (zoom of Figure 9) of the raveling test conducted along the left bank and recorded by the geophone A.

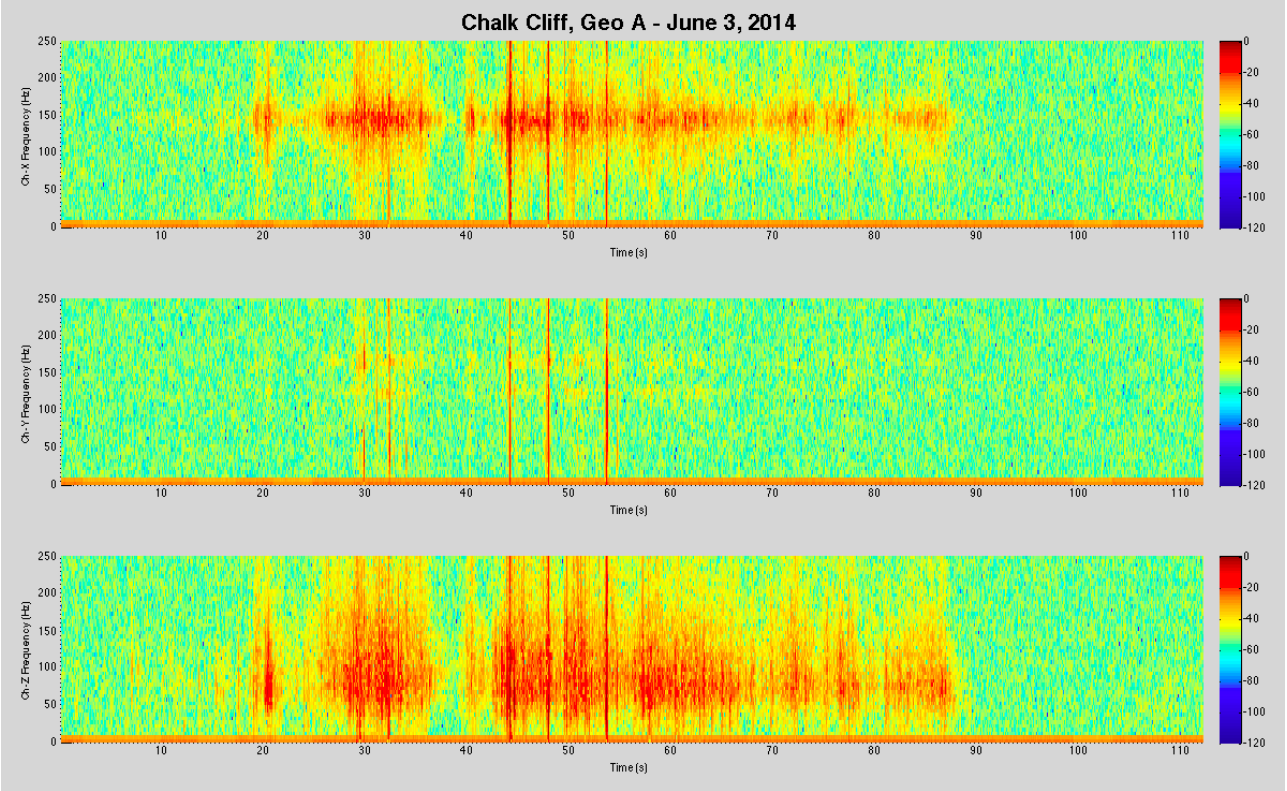

Figure 11 - The spectrogram of the raveling test conducted between 12:36:55 and 12:38:10 (section 4) and recorded by the geophone A.

Data Analysis

1. Irregular sampling rate

Analyzing data, a malfunctioning in the timing of the recordings has been found. The theoretical sampling rate set on the data logger is 500 Hz but during the acquisition the system performs a drop of some samples with a pretty regular time interval (Figure 12). Only 467 samples per seconds are on the average recorded; as a consequence, some details of the spectral analysis presented before have to be reviewed. In particular, the time scale on the x-axis is actually wider, i.e. the x limits of Figure 11 should be 0-120 seconds.

Performing frequency analysis of a dataset affected by a non-uniform sampling rate is possible; in some cases the latter can even have a positive anti-aliasing effect (Figure 13). In our case we have some drops in time but apart from that when the recording properly works the dataset has a uniform scan rate of 2 msec. This problem is likely due to the high number of samples per seconds recorded by the data logger (500 Hz per channel per sensors = 3000 Hz). Indeed, on the 5 V range code, with minimal processing, measurement rates up to 2000 Hz on a single channel can be achieved by the CR5000. As a consequence, the sampling rate will be reduced to 250 Hz (equals to 1500 Hz for the whole system) to ensure a correct recording.

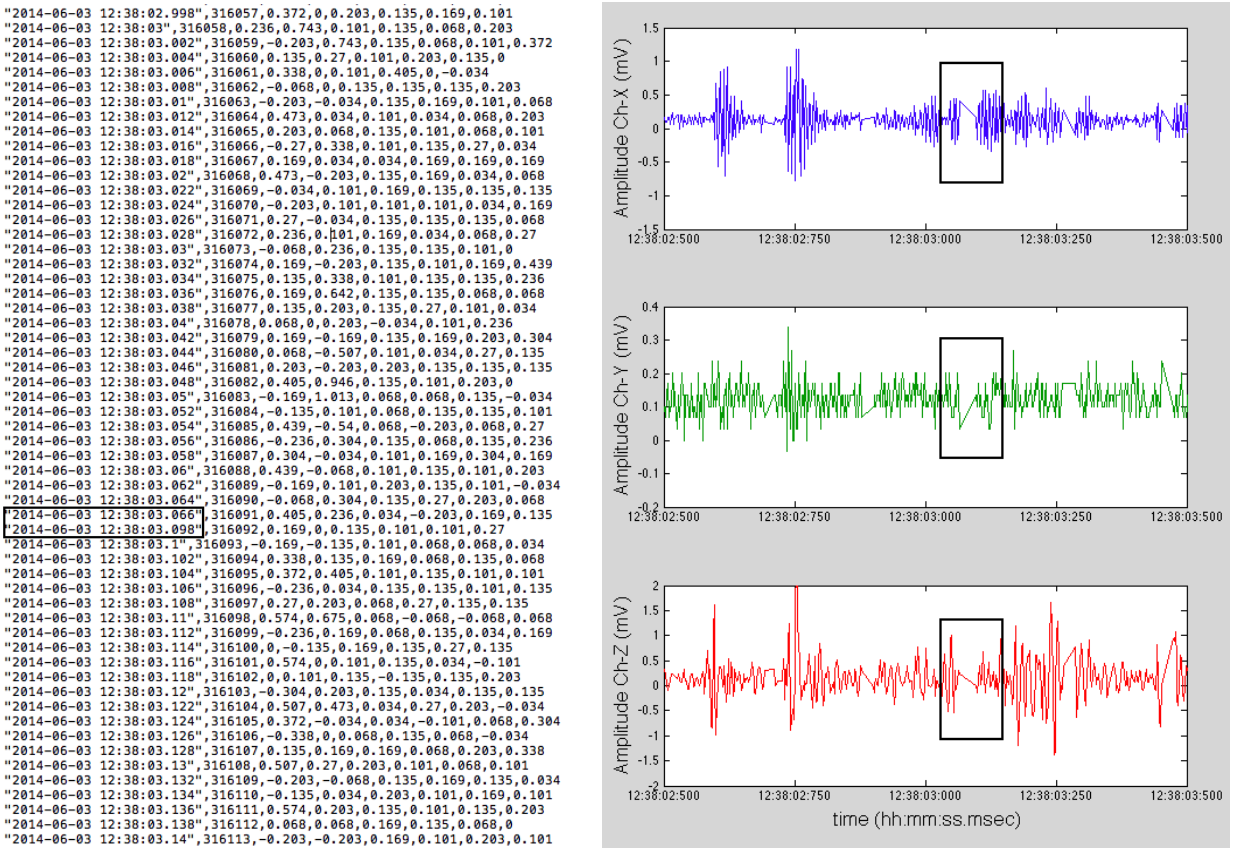

Figure 12 – The data logger irregular sampling rate, the values recorded on June 3 on the left and the geophone A graphs on the right. A drop example is highlighted in the black frames.

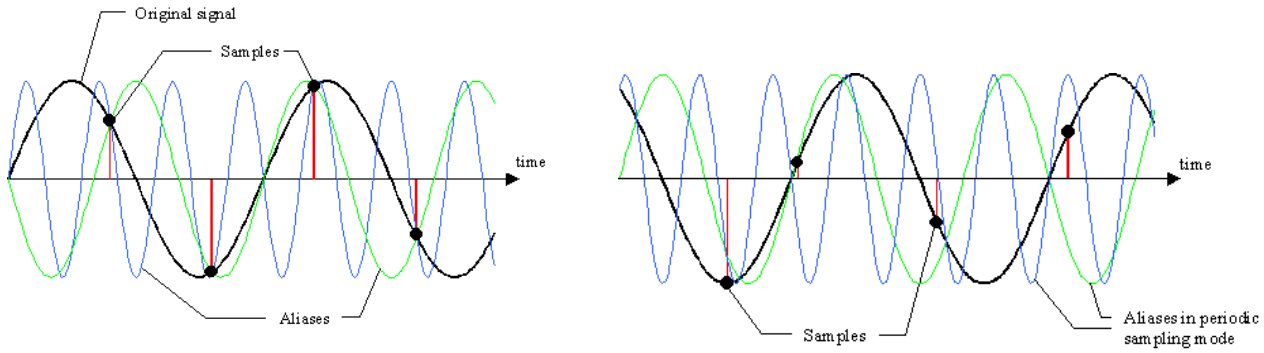

Figure 13 – On the left, aliasing effect in the case of a periodic sampling, on the right only one sine function goes exactly through the non-uniformly spaced sample values (images after www.edi.lv).

2. Background-sampling rate

For the definition of an appropriate background-sampling rate, the signals showed in Figure 8 and 10 have been subsampled at 10, 50 and 100 Hz. The results presented in the Figure 14 and 15 show that with a sampling rate of 10 Hz the waveforms are compromised while recording at 100 Hz the signals are pretty similar to the original ones recorded at a sampling rate of 500 Hz. The intermediate frequency of 50 Hz would be an acceptable compromise.

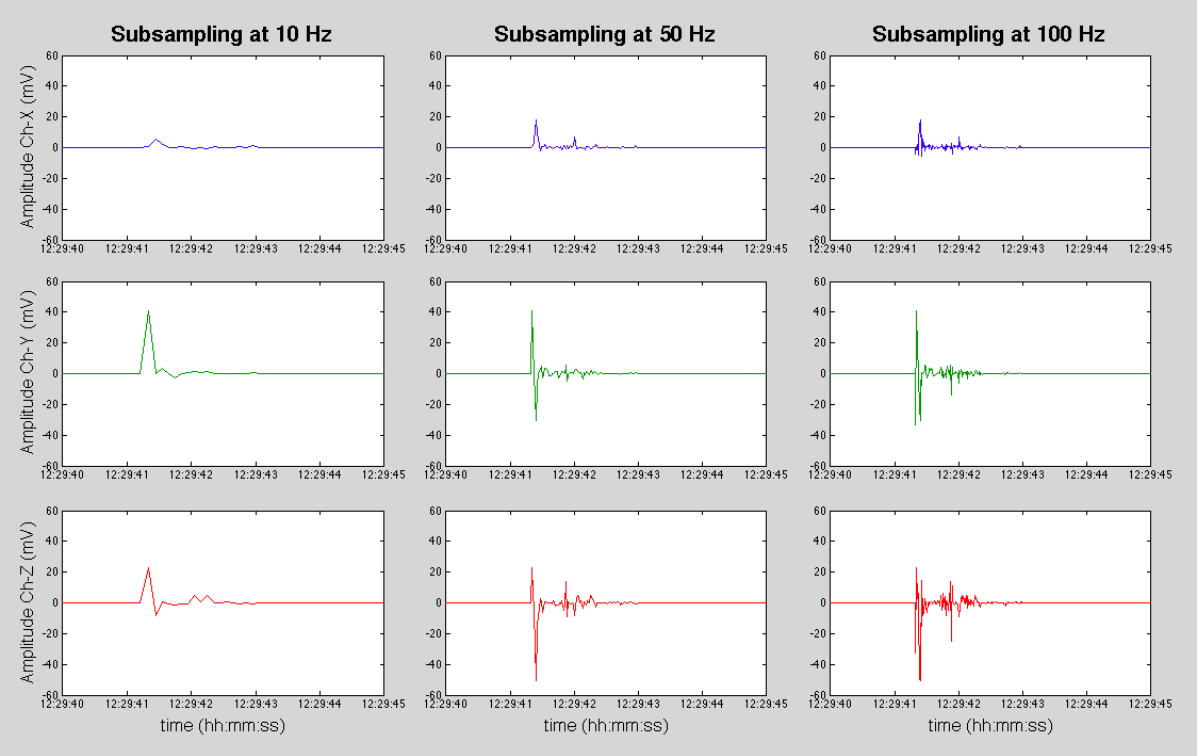

Figure 14 – The signal related to the rock fall test conducted on the right bank (section 2) on June 3, 2014 subsampled at 10, 50 and 100 Hz. The original signal recorded at a sampling rate of 500 Hz is showed in Figure 8.

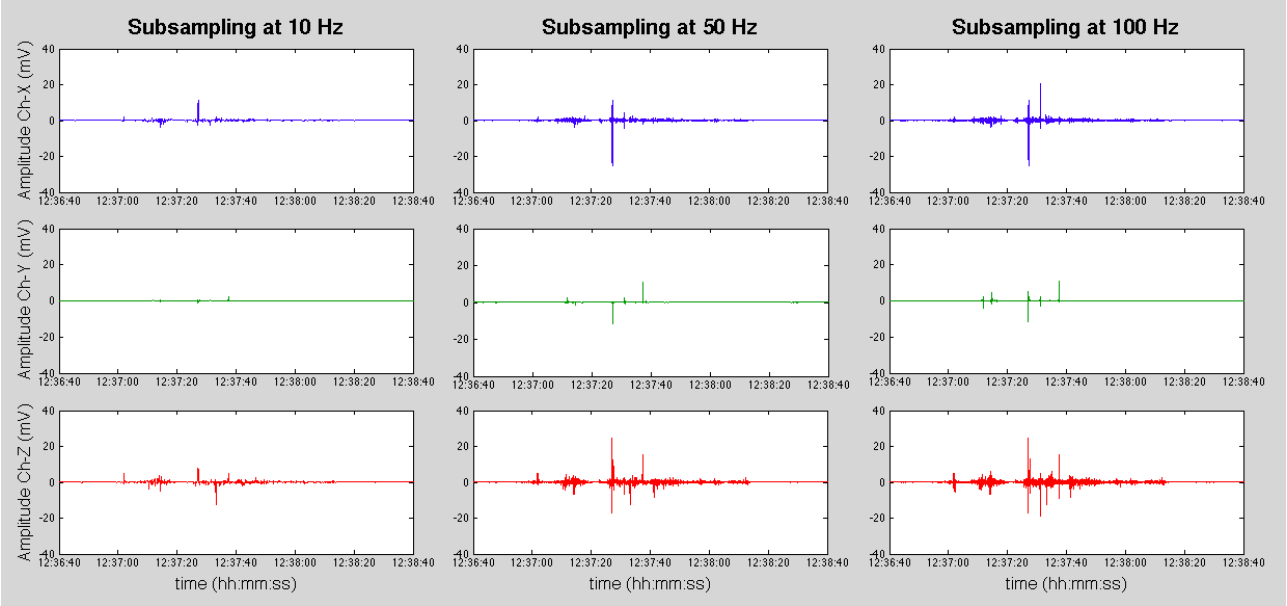

Figure 15 – The signal related to the raveling test conducted on the left bank (section 4) on June 3, 2014 subsampled at 10, 50 and 100 Hz. The original signal recorded at a sampling rate of 500 Hz is showed in Figure 10.

3. On the definition of a recording threshold

Working at a high sampling rate, the sensors will be likely able to detect small mass movement like those simulated in the presented tests from a distance of few tens of meters. Of course larger mass movements occurring at a higher distance are expected to be detected. Both geophones seem to properly work in correspondence of the section where they are installed, detecting the impacts and the movements occurring in the restricted areas surrounding them. In particular, geophone A appears to be slightly more sensitive, detecting higher vibration values during rock fall and raveling simulations conduced on the left bank. Apart from the distance source/receiver, this difference could be related to the different installation conditions of the two sensors. The geophone mentioned before is screwed on the vertical face of a stable block located on the left bank of the channel. On the contrary, the other sensor is installed on the right bank, composed by highly fractured rocks. Concerning the different geophone axis, both sensors are more sensitive on the vertical axis. The latter can be used as a reference for triggering the recordings in fall and winter seasons, when debris flows do not occur but rock falls do. Considering the background noise and the amplitude values summarized in Figures 6 and 7, a threshold value included in the range 2-4 mV can be adopted for geophone A, while a threshold equals to 1 mV can be used for geophone B.

References

Coe, J. A., Kinner, D. A., & Godt, J. W. (2008). Initiation conditions for debris flows generated by runoff at Chalk Cliffs, central Colorado. Geomorphology, 96(3), 270-297.